Available online at www.sciencedirect.com
SCIENCE DIRECT
Journal of Chromatography B, 829 (2005) 115–122
JOURNAL OF CHROMATOGRAPHY B
www.elsevier.com/locate/chromb

# Micellar electrokinetic capillary chromatography reveals differences in intracellular metabolism between liposomal and free doxorubicin treatment of human leukemia cells

Angela R. Eder, Edgar A. Arriaga *

*Department of Chemistry, University of Minnesota, Minneapolis, MN 55455, USA*

Received 8 February 2005; accepted 30 September 2005
Available online 21 October 2005

**Abstract**

Doxil® is a pegylated liposome formulation of the anthracycline doxorubicin. To better explain observed differences in the toxicity of Doxil® and free doxorubicin in solution, the intracellular metabolism of the formulations after treatment in CCRF-CEM and CEM/C2 human leukemia cell lines was investigated. Using micellar electrokinetic capillary chromatography with laser-induced fluorescence detection, with a 63 zepto ($10^{-21}$) mole doxorubicin limit of detection, five common metabolites and doxorubicin were detected upon treatment with both of these drug delivery systems. Two unique metabolites appeared with the Doxil® and two unique metabolites appeared with the free doxorubicin delivery systems. For common metabolites, the relative amount of metabolite generated from Doxil® was approximately 10 times higher than for free doxorubicin.


*Keywords:* Doxorubicin; Doxil; Liposome; Micellar electrokinetic capillary chromatography; Capillary; Electrophoresis; Laser-induced fluorescence; Metabolism

## 1. Introduction

Despite wide spread clinical utilization in the treatment of cancer, the efficacy and utility of the anthracycline doxorubicin (DOX) continues to be hampered by the onset of dose-dependent cardiotoxicity and acquired multi-drug resistance (MDR) [1]. It is believed that the MDR and cardiotoxic phenotypes are linked with the subcellular metabolism of this drug through enzymatic pathways that, to date, have not been fully elucidated, despite extensive study [2–4].

Various delivery systems have been explored in an attempt to better target DOX to malignant tissue and improve therapeutic regimens [5], which would lead to decreased cytotoxicity to healthy tissues [2]. These include micelles, polymer linkers [2], prodrugs, microspheres [6], and liposomes [7]. Currently, liposomes are being utilized clinically as a chemotherapy agent (Doxil®). Extensive clinical studies have indicated that the incorporation of a liposome in the drug formulation has drastically altered the pharmacokinetic parameters of treatment, leading to increased drug accumulation in tumors and a reduction of side effects. Benefits of such a system include greater drug payload to malignant tissue [8]; decreased incidence of alopecia, myelosuppression, and cardiotoxicity [5,9]; and partial reversal of MDR phenotypes in in vitro systems due to the high intraliposomal concentrations of DOX (∼200 mM) [2,10]. While clinical studies have provided physiological explanations for differences in the pharmacological profiles of liposome formulations compared to free drug in solution, only one study to date has been conducted on the metabolism of liposome formulations of anthracyclines in plasma [18]. Missing in these studies is a metabolic explanation for differences in toxicity observed between the liposome and free drug formulations of DOX, particularly in the context of intracellular metabolism.

Previous research has implicated the intracellular accumulation of DOX metabolites in many of the side effects and decreased efficacy seen after intravenous treatment [11]. For instance, one of the primary mechanisms by which DOX exerts cytotoxic effects is to form a ternary complex with DNA and Topoisomerase II-α, thereby arresting DNA synthesis and resulting in cell death [12–14]. However, formation of this ternary complex with the main metabolite, doxorubicinol (DOXol), and aglycone metabolites is less stable when compared to that of

* Corresponding author. Tel.: +1 612 624 8024; fax: +1 612 626 7541.
*E-mail address:* arriaga@chem.umn.edu (E.A. Arriaga).

1570-0232/$ – see front matter © 2005 Elsevier B.V. All rights reserved.
doi:10.1016/j.jchromb.2005.09.038

the parent compound, resulting decreased therapeutic efficacy caused by the decreased stability of the ternary complex [15]. Furthermore, DOX has been shown to suppress respiration in mitochondria; respiration is even further suppressed by aglycone metabolites [16].

Others have investigated the metabolism of DOX in plasma using HPLC [17–19]. However, this approach is limited, since the majority of DOX metabolites are present at concentrations <1% of the parent compound [20]. While these molecules retain native fluorescence, the sensitivity of HPLC would require a significant increase in the amount of cellular sample. Capillary electrophoresis with laser-induced fluorescence detection (CE-LIF) offers low injection volume (∼1 nL) and extraordinarily low limits of detection (∼60 zmol or 60 pM for DOX) [21] that will allow for the analysis of these low abundance metabolites with relative ease. Previous analyses using micellar electrokinetic capillary chromatography (MEKC) with LIF detection has resulted in the detection of as many as 11 sub-attomole DOX metabolites in cultured cells [20–22].

We are reporting on the use of CE-LIF to probe the impact of drug delivery system (liposomes versus "free" DOX in solution) on the metabolite formation in whole cell lysate of a parent (CCRF-CEM) and derived (CEM/C2) cell line. These pair of related human leukemia lines are considered to be a better model than previously used murine cell lines because, due to the species specificity of DOX metabolism, they will more closely resemble the drug's metabolism in the treatment of leukemia [23,24]. This report provides the first electrophoretic separation of a commercial DOX liposome preparation and the first investigation of the impact of drug delivery on intracellular metabolism by CE-LIF.

## 2. Experimental

### 2.1. Chemicals and reagents

DOX was donated by Dr. A. Suarato (Pharmacia, Nerviano, Italy). Doxil® was purchased from Alza (Mountain View, CA). Sodium borate decahydrate was purchased from EM Science (Gibbstown, NJ, USA). Sodium dodecyl sulfate (SDS) Ultrapure Bioreagent was purchased from J.T. Baker (Phillipsburg, NJ, USA). Methanol (MeOH) was purchased from Pharmco (Brookfield, CT, USA). γ-Cyclodextrin (CD), a stock solution (10×) of phosphate buffered saline (137 mM NaCl, 2.7 mM KCl, 10 mM $Na_2HPO_4/KH_2PO_4$, pH 7.4) (PBS) and 0.4% Trypan Blue solution were purchased from Sigma Aldrich (St. Louis, MO, USA). All buffers were made using 18 MΩ water obtained from a Millipore water purification system (Billerica, MA, USA). The pH of all buffers and solutions was adjusted using either 0.1 M HCl or 0.1 M NaOH after the addition of solutes. Following pH adjustment, buffers were filtered through a 0.22 μm Nalgene filter and stored at room temperature for up to 1 month. MEKC buffer consisted of 10 mM borate, 10 mM SDS at pH 9.37 (BS buffer), above the critical micellar concentration (cmc) of SDS in 10 mM borate [25]. CD-MEKC buffer consisted of 20 mM γ-CD, 50 mM borate, 50 mM SDS at pH 9.3 (CD-BS buffer).

Stock solutions of DOX were prepared in 100% MeOH at $1.0 \times 10^{-3}$ M. The stock solutions were stored at −20 °C and used up to 1 month post-preparation. Working solutions were prepared on the day of analysis to prevent repeated freeze–thaw cycles of the stock.

### 2.2. Cell culturing

Passages 17 and 18 of CCRF-CEM and CEM/C2 human leukemia cells (American Type Culture Collection (ATCC), Manassas, VA, USA), cultured at 37 °C and 5% $CO_2$ in RPMI 1640 media (ATCC), supplemented with 10% bovine calf serum (Invitrogen Corp., Carlsbad, CA, USA) were used in these studies. The cells were maintained by splitting every 3–4 days through the addition of fresh media; treatment began 10 h after splitting. Dosages of 25 μM DOX in solution (free DOX) or Doxil® (equivalent to 50 μM DOX) were determined to have comparable viabilities (i.e. >80% by Trypan Blue exclusion, 12 h after the initiation of treatment). For control experiments in which cells were not treated, cell culturing protocols remained identical. Biosafety Level 1 was observed for all culturing and preparations.

### 2.3. Sample preparation

Cells were pelleted by centrifugation ($2000 \times g$ for 20 min.) with an Eppendorf microcentrifuge (Brinkman Instruments, Westbury, NY, USA) and washed twice by resuspending in 1× PBS buffer following treatment. Cells were then dissolved to a density of $2 \times 10^6$ cells/mL in BS buffer and divided into triplicates. In addition to its utilization as a MEKC buffer, the BS buffer facilitates disruption of cellular membranes, making it possible to directly sample the lysate was without further preparative steps.

### 2.4. CE-LIF set-up and analysis

MEKC of whole cell lysate was performed using a home-built instrument previously described [26]. High voltage was applied from a CZE1000R high voltage power supply (Spellman, Hauppauge, NY, USA). Samples were introduced by electrokinetic injections of +100 V/cm for 5 s, and were separated at +400 V/cm using uncoated fused-silica capillaries (50 μm i.d. and 150 μm o.d.) (Polymicro Technologies, Phoenix, AZ, USA). Running buffer was changed after each run to minimize buffer depletion and to reduce the possibility of contamination from one sample to the next. The capillary was conditioned after analysis of all the replicates of a given sample by consecutively flushing the capillary under constant pressure of 100 kPa for 2 min each with MeOH, 0.1 M NaOH, $H_2O$, 0.1 M HCl, $H_2O$, BS buffer, followed by three injections of the same sample. The last step was necessary to increase reproducibility of peak areas and migration times for peaks in subsequent injections of the sample. The capillary was not conditioned between injections, as this was not found to increase reproducibility (data not shown).

To decrease the background caused by the polyimide coating, 2 mm of this coating were burned off at the detection end of the capillary. This capillary end was placed in the sheath flow cuvette of the post-column detection system. The 488 nm line

of an Argon ion laser (JDS Uniphase, San Jose, CA, USA) was used for excitation of fluorescent analytes. Fluorescence emission from species migrating out of the capillary was collected at 90° with respect to the excitation beam by a 60× microscope objective (Universe Kogaku, Inc., Oyster Bay, NY, USA) [21]. Scattering from bubbles and/or contaminants in the samples at 488 nm was further reduced spectrally and spatially with a 505 nm long-pass filter (Omega Optical, Brattleboro, VT, USA) and a 1.4 mm pinhole. A 635 ± 27.5 nm bandpass filter (model XF3015, Omega Optical, Brattleboro, VT, USA) was then used to select the emission spectra for DOX [21].

Prior to carrying out any sample analysis, the detector was aligned by continuous injection of $10^{-9}$ M fluorescein in BS buffer at +400 V/cm and optimizing the position of the capillary end relative to the laser and detector in order to maximize the response of the photomultiplier tube (R1477, Hammamatsu, Bridgewater, NJ, USA) biased at 1000 V. After the alignment, the limit of detection (S/N = 3) was estimated to be 3 zmol from electrokinetic injections of $10^{-10}$ M fluorescein. A 535 ± 17.5 nm bandpass filter (model XF3007, Omega Optical, Brattleboro, VT, USA) was used instead of the doxorubicin filter described above.

### 2.5. Data collection

The PMT output current was measured across a 1.0 MΩ resistor. As a result, the PMT signal and fluorescence intensities are reported in volts (V). The PMT output was collected at 50 Hz using a data acquisition board and run with an in-house Labview (National Instruments, Austin, TX, USA), program and stored as a binary file. Data were smoothed with a 10 point Median Filter and 10 point binomial smoothing in Igor Pro (Wavemetrics, Lake Oswego, OR, USA). A calibration curve was constructed using DOX standards in order to estimate the amount of DOX and metabolites produced in each cell line. While the quantum yield of the metabolites is slightly different than that of the parent compound, the similarity in emission spectra and quantum yield allows for estimation of metabolites present in a sample by comparing peak area to that of a DOX standard [27]. By comparing DOX molar concentration, [DOX], to DOX peak area, $A_{DOX}$, the following equation was obtained:

$$A_{DOX} = (1.00 \pm 0.04) \times 10^8[DOX] - (2.0 \pm 0.1) \quad (1)$$

The linear range of this equation was $10^{-10}$ to $10^{-6}$ M with $r^2 = 0.993$.

The electrophoretic mobility was calculated as:

$$\mu_a = \frac{L_t^2}{t_m E} \quad (2)$$

where $L_t$ is the length of the capillary, $t_m$ the migration time of the analyte, and $E$ is the applied electric field during the separation.

From the calculated electrophoretic mobility, a corrected mobility was determined based on a metabolite peak that was selected as a reference peak, and that appeared in all the sample electropherograms (see Section 3). For each run, the electrophoretic mobility axis was corrected by multiplying the calculated mobility by a factor that resulted in matching the mobility of the reference peak in the run to the average mobilities of this peak in all runs. This correction procedure was based on previously reported procedures used for correcting migration times in capillary electrophoresis [28,29].

### 2.6. Statistical analysis

A one-tailed *t*-test, assuming equal sample variance, was performed using Microsoft Excel. The adjusted mobility values of all peaks were compared between samples. For all *t*-tests, the null hypothesis "there is no difference in the adjusted mobility values" was tested at a confidence interval ($P$) of 98%. The null hypothesis was rejected when $P < 0.02$.

## 3. Results and discussion

### 3.1. Electropherogram reproducibility

Previous studies have reported that several injections of a DOX standard prior to the analysis of the sample improve electropherogram reproducibility [20]. The need to include DOX injections as part of the conditioning protocol prior to sample analysis suggests that the capillary walls also participate in the determination of the electrophoretic mobility. In fact, one of the drawbacks in the analysis of biological samples by MEKC is the possible interaction of the biological matrix with the capillary walls, modifying the electroosmotic flow and the interactions of the analytes with the walls. Since it is not known the extent to which cellular components found in the cell lysate modify the capillary walls and contribute to the observed electrophoretic mobilities of the various peaks, the use of sample injections as part of conditioning protocol was investigated. This approach is considered to be more adequate than conditioning with injections of a DOX standard as previously reported [20], because it decreases the possible exchange of DOX bound to the capillary surface with sample components and prevents overestimation of fluorescent components in the sample resulting from this exchange.

By plotting relative standard deviation of peak area and migration time versus injection number, it was found that reproducibility increased after with subsequent injections (e.g. first to third injection) and then it stabilized (Fig. 1), indicating that the capillary wall was fully conditioned for sample analysis. Further injections did not reveal a clear enhancement in the reproducibility of these parameters. SDS concentrations higher than 10 mM did not improved the reproducibility of the separation (data not shown). It appears that the interaction between the sample components (e.g. proteins) and the capillary surface are strong enough that the used SDS was not able to disrupt this interaction. This is not surprising, as protein adsorption to silica surfaces (e.g. capillary wall) is well documented, even in the presence of SDS [30,31]. Therefore, a correction procedure was used to further enhance reproducibility.

The R.S.D. values for the calculated electrophoretic mobility of each peak in the various samples (Fig. 2) were as high as 3.5%. By using peak 6 (cf. Fig. 1) as a reference, and correcting the

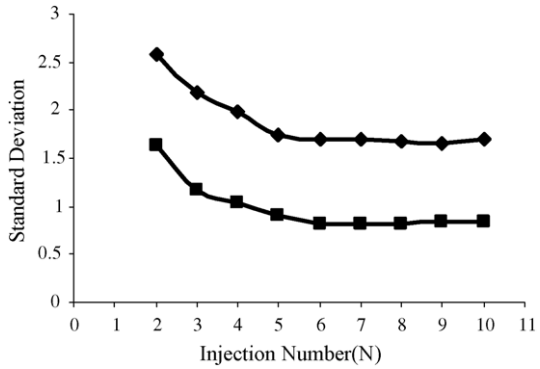


Fig. 1. Change in the standard error for the migration time with consecutive injections. CCRF-CEM cells were treated with free DOX (♦) and Doxil® (■) as indicated in Section 2. Only a peak arbitrarily assigned as #6 is represented.

electrophoretic mobility scale by a factor that resulted in matching this peak's electrophoretic mobility to the average value in all the analyzed samples, a corrected electrophoretic mobility was calculated for each peak in each sample. The R.S.D. for these corrected electrophoretic mobilities are shown in Fig. 2, and demonstrate that, overall, R.S.D. has decreased. In some instances, there was no clear improvement when this correction was applied (i.e. metabolites 1 and 2 in Fig. 2A and metabolites 8 and 10 in Fig. 2D). This is expected because the same correction factor may not be adequate when different mechanisms contribute differently to the migration time of these components in the sample. If an adequate fluorescent micellar marker, excitable at 488 nm were available, this marker would help further refine the procedure for correcting the electrophoretic mobility by taking into account the variations in the electrophoretic mobility of the micelles. Unfortunately, previously reported micellar markers are either non-fluorescent (e.g. Sudan Red III) [32] or its fluorescent properties (e.g. Halofantrine) [33] are not appropriate for the detection conditions described in this work.

With the enhancement in reproducibility demonstrated in Fig. 2, it was possible to compare and contrast the effect of drug delivery system on the metabolism of DOX, as well as provide a comparison of the effect of Doxil® treatments on both cell lines. A *t*-test of corrected electrophoretic mobility indicates that all but two peaks, 5 and 6, were statistically different from each other. Other on-going studies to improve the reproducibility in migration times and electrophoretic mobilities are the inclusion of fluorescein as an internal standard for mobility correction, and the use of protein precipitation and/or saponification to remove cellular materials that might influence micellar properties.

### 3.2. Comparison of electrophoretic profiles

Fig. 3, trace (i), shows a representative electropherogram of the Doxil® preparation. Prior to analysis, the Doxil® formulation was solubilized in BS buffer for 1 week at 4 °C, followed by sonication. Other attempts at solubilizing the Doxil® formulation with BS buffer for 48 h prior to analysis resulted in poor migration time, peak intensity, and peak area reproducibilities. The need of the extended solubilization period prior to attaining reproducibility is in agreement with the high stability of Doxil® [34] that typically requires hyperthermia, sonication, an acidic environment, or a combination of all three environments to facilitate liposome disruption [9,35,36]. DOX has been shown to form aggregates in the aqueous intraliposomal region, which is stabilized by $\pi$–$\pi^*$ interactions [37,38]. Furthermore, DOX has been shown to form stable complexes with a variety of lipids and proteins [39,40]. These interactions may explain the complex profiles observed in Fig. 3(i) (peaks 1′–6′). The peak at $2.9 \times 10^{-4}$ cm$^2$ V$^{-1}$ s$^{-1}$ is associated with free DOX, while peaks 1′–6′ may be associated with the DOX-phospholipid complexes [41,42].

A *t*-test comparing the corrected electrophoretic mobilities of the peaks in the electropherograms of the Doxil® standard and the lysate from CCRF-CEM cells treated with Doxil® (Fig. 3(i)

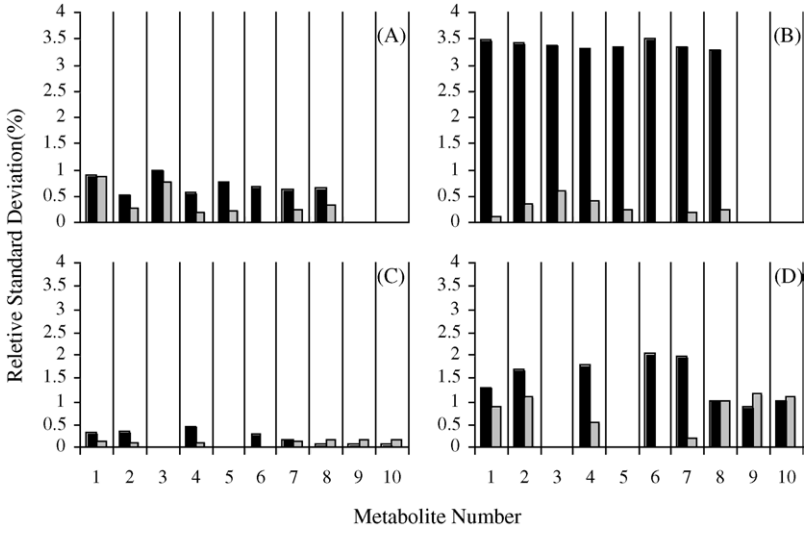


Fig. 2. Mobilities for free DOX (A and B) and Doxil (C and D) are shown for metabolites found in CEM/C2 (A and C) and CCRF-CEM (B and D) lysates. The *x*-axis refers to an arbitrary numbering system used for identification purposes in these studies. Three replicates are included in this study.

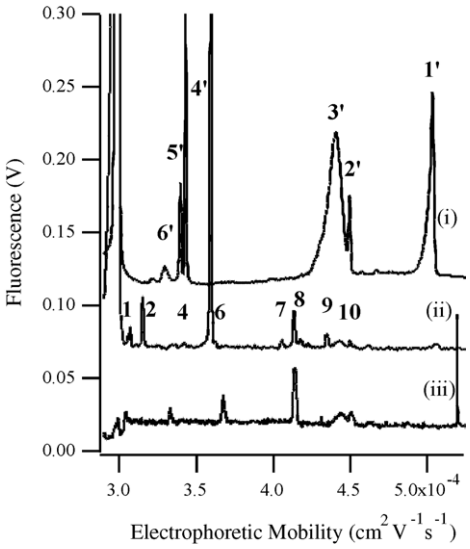


Fig. 3. Comparison of Doxil® formulation and treatments. (i) Doxil® formulation was solubilized by BS buffer for 1 week at 4 °C, followed by sonication (peaks 1′–6′). (ii) Doxil® treated CCRF/CEM cell lysate (peaks 1, 2, 4, 6–10). (iii) Untreated CCRF/CEM cell lystate. Treatment of cells with Doxil® consisted of a 12 h treatment with an equivalent dose of 50 μM drug. Separation was performed at +400 V/cm in an uncoated capillary. Doxil® samples were injected for 5 s at +50 V/cm. Cellular samples were injected for 5 s at +100 V/cm. BS buffer was used as the running buffer and sample buffer. Trace (i) has been reduced in intensity by 25% in order to keep trace in scale. Traces (i) and (ii) have been offset in the *y*-axis for clarity.

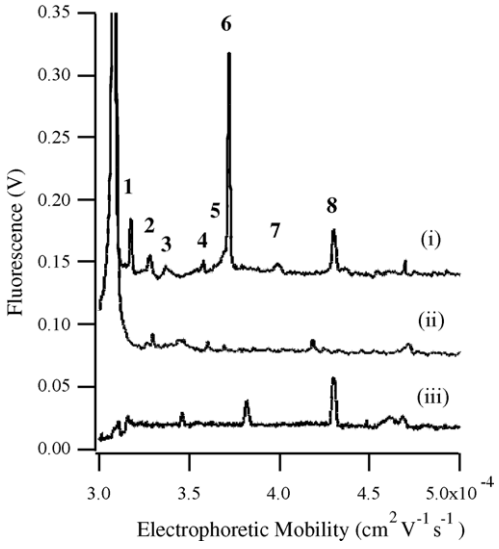


Fig. 4. Comparison of free DOX metabolism and free DOX in media. (i) CCRF-CEM cells were treated with 25 μM free DOX for 12 h. (ii) A control of free DOX after 12 h incubated in sterilized media without cells. (iii) Untreated CCRF-CEM cell lysate. DOX from incubated media was injected for 5 s at +50 V/cm. Otherwise, injection and separation conditions can be found in Fig. 3. Traces (i) and (ii) have been offset in the *y*-axis for clarity.

and (ii), respectively) reveals that there are no coincident peaks between the two samples at the 98% confidence interval, indicating that peaks in the profile of treated cell lysate cannot be attributed to the Doxil® formulation. The same conclusions were drawn from the treatment of CEM/C2 cell lines with Doxil® (data not shown). It is interesting that the peaks associated with the Doxil® formulation are not detectable in the electropherograms of Doxil® treated cellular samples. It is possible that, upon entering the cell via pinocytosis, Doxil® components are fully solubilized by the low pH associated with acidic organelles. This explanation is consistent with the observation that liposomes destabilize and solubilize after pinocytosis [43]. Therefore, it can be assumed that the remaining peaks in Fig. 3, trace (ii), except for peak 8, are likely the result of DOX metabolism.

Before identifying metabolite peaks resulting from treating either CCRF-CEM or CEM/C2 cells with one of the two drug delivery systems, a control consisting of untreated cells was analyzed by MEKC-LIF. Peak 8 was detected at an adjusted mobility of $4.3 \times 10^{-4}$ cm$^2$ V$^{-1}$ s$^{-1}$ in the untreated controls (Fig. 3(iii) or Fig. 4(iii)). While previous research has not detected the presence of autofluorescence in this pair of cell lines [20], comparison of this control with other traces corresponding to treated samples (Figs. 3(ii) and 4(i)) indicated that peak 8 is the result of autofluorescence of cellular components and not from metabolism.

Upon treatment with of the CCRF-CEM cell line with free DOX or Doxil®, transformation of the parent DOX product was observed (Figs. 3(ii) and 4(i), respectively). Free DOX treatment leads to the appearance of metabolites (1–7). On the other hand, Doxil® treatment leads to the appearance of metabolites (1, 2, 4, 6, 7, 9 and 10) (Fig. 3(ii)). These metabolites are clearly different from the profiles resulting from the analysis of DOX standard or the Doxil® preparation alone (Figs. 4(ii) and 3(i), respectively). The same metabolic profiles after treatment with free DOX or Doxil® was observed for the CEM/C2 cell line (data not shown). These data clearly show that metabolism is dependent on the method of drug delivery.

The two delivery systems (Fig. 5) show five common peaks associated with metabolism (peaks 1, 2, 4, 6 and 7) in the

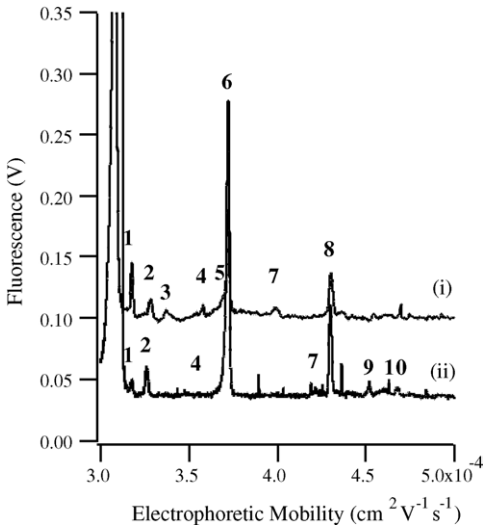


Fig. 5. Free doxorubicin vs. Doxil® metabolism. CCRF-CEM cells were treated with (i) 25 μM free DOX (ii) 50 μM (equivalent DOX) Doxil® for 12 h. The metabolite numbering system has been indicated above traces (i) and (ii). Peak 7 displayed high variability in this separation system. Traces have been offset in the *y*-axis for clarity. Separation conditions can be found in Fig. 3.

electrophoretic profiles resulting from metabolite formation in CCRF-CEM cells. Fig. 5 also shows the differences in profiles resulting from the treatment with free DOX (trace (i)) and Doxil® (trace (ii)). Metabolites 3 and 5 were present in free DOX treated cells but not present in Doxil® treated samples; metabolites 9 and 10 were present in Doxil® treated cell but absent from free DOX treated cells. Statistical analysis of the corrected mobilities revealed that metabolites 5 and 6 were not statistically different at the 98% confidence level, as were the remaining metabolites. Therefore, peak identification of these metabolites relied on both corrected mobility, peak position, and shape.

Doxorubicinol (DOXol) has been considered the primary metabolite of DOX in human plasma and urine [2,17]. This metabolite cannot be resolved from DOX in the BS buffer system used for the other metabolites. On the other hand, use of the CD-MEKC system than can separate DOXol from DOX, demonstrated that the CCRF-CEM and CEM/C2 cell lysates, from cell treated with DOX and Doxil®, did not have detectable DOXol (data not shown).

The abundance of DOX metabolites in the two drug delivery systems was also compared. Average metabolite abundance for each delivery systems and cell line can be found in Table 1. Based on peak area, the absolute metabolite abundance showed no differences in at the 98% confidence level for a given metabolite in comparisons between drug delivery system for a given cell line (i.e. Doxil® treated CCRF-CEM versus free DOX treated CCRF-CEM), In contrast, the amount of DOX accumulating in Doxil® treated cells was significantly lower than in free DOX treated cells. The relative (percent) metabolite abundance with respect to total DOX abundance in the two delivery systems is shown in Fig. 6. These data reveal that, in both cell lines, the percent metabolite concentration is significantly higher in Doxil® treated cells than free DOX treated cells.

Similar absolute amounts of metabolites for both drug delivery systems and higher relative abundance for the Doxil® treated cells may be an indication that the enzymatic pathways involved in DOX metabolism are saturated under free DOX treatment [44]. It could also be that the majority of DOX metabolism is occurring in acidic organelles, as opposed to the cytosol as previously believed (e.g. carbonyl reductase, NADH dehydrogenase) [2]. Based on the reported p$K_a$ for DOX, it is possible to calculate that approximately 9% of free DOX is taken up through pinocytosis, while the remaining drug is taken up by cells through passive diffusion [1,45]. Conversely, liposomes only deliver their drug payload to a cell when taken up by

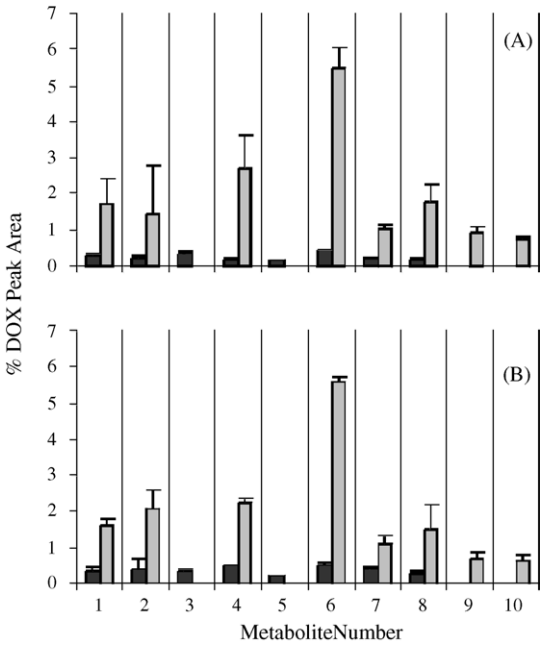


Fig. 6. Relative abundance of metabolites in free DOX and Doxil® treated cells. Metabolite accumulation is expressed as percent DOX peak area for DOX treated (black) and Doxil treated (gray) CCRF-CEM (A) cells and DOX (black) and Doxil treated (gray) CEM/C2 (B) cells. Error bars represent the standard deviation of three replicate injections.

Table 1
Average electrophoretic mobilities and abundance in moles per cell as determined by peak area for metabolites resulting from treatment of CCRF-CEM or CEM/C2 cells with either free DOX or Doxil® ($n = 3$)

| Metabolite[a] | Mobility[b] | Moles per cell[c] | | | |
|---|---|---|---|---|---|
| | | CCRF-CEM free DOX | CEM/C2 free DOX | CCRF-CEM Doxil® | CEM/C2 Doxil® |
| 1 | 3.21 ± 0.06 | 0.60 ± 0.01 | 0.60 ± 0.02 | 0.72 ± 0.03 | 0.72 ± 0.01 |
| 2 | 3.29 ± 0.05 | 0.59 ± 0.01 | 0.60 ± 0.05 | 0.74 ± 0.04 | 0.74 ± 0.02 |
| 3 | 3.33 ± 0.04 | 0.60 ± 0.01 | 0.60 ± 0.01 | N/A | N/A |
| 4 | 3.56 ± 0.06 | 0.57 ± 0.01 | 0.63 ± 0.01 | 0.77 ± 0.04 | 0.75 ± 0.002 |
| 5 | 3.67 ± 0.04 | 0.57 ± 0.002 | 0.58 ± 0.01 | N/A | N/A |
| 6 | 3.75 ± 0.06 | 0.64 ± 0.002 | 0.63 ± 0.01 | 0.89 ± 0.03 | 0.90 ± 0.01 |
| 7 | 4.12 ± 0.18 | 0.58 ± 0.01 | 0.61 ± 0.01 | 0.69 ± 0.01 | 6.95 ± 0.11 |
| 8[d] | 4.33+0.08 | 0.57 ± 0.01 | 0.59 ± 0.01 | 0.73 ± 0.02 | 0.71 ± 0.03 |
| 9 | 4.63+0.04 | N/A | N/A | 0.68 ± 0.01 | 0.68 ± 0.01 |
| 10 | 4.79 ± 0.04 | N/A | N/A | 0.68 ± 0.003 | 0.67 ± 0.01 |
| DOX | 3.14 ± 0.03 | 141.59 ± 4.45 | 119.96 ± 1.91 | 15.99 ± 0.31 | 16.19 ± 0.32 |

[a] Metabolite numbering system is the same as in Fig. 5. Data correspond to the average of triplicate injections. Variation is represented in standard deviation.
[b] Electrophoretic mobility/$10^{-4}$ ($cm^2\ V^{-1}\ s^{-1}$); average mobility calculated from individual electrophoretic mobilities from every injection in every sample.
[c] Metabolite amount was calculated from the average peak area, the DOX calibration curve, and the total number cells ($2.0 \pm 0.4 \times 10^6$ cells/mL). Estimated content per cell ($\times 10^{-19}$) determined from Eq. (1).
[d] Detected in untreated (blank) cell lysate; therefore, this peak is not considered to be the result of metabolism.

pinocytosis. Since a higher percentage of DOX was metabolized in Doxil® treated cells, the logic follows that the metabolism must be occurring in acidic organelles, the organelles responsible for pinocytosis. Conversion of DOX in acidic organelles may be indicative of chemical conversion through acid hydrolysis [27].

Alternatively, the higher relative abundance of metabolites attributed to Doxil® treatment could be the result of decreased aglycone removal through drug efflux pumps located in the plasma membrane as a result of bypass of these membranes during drug uptake. For example, co-elution studies have indicated that peaks 1-8 may be aglycone metabolites of DOX [20], which are thought to have a high affinity to the efflux pump P-glycoprotein (Pgp) [46]. In Doxil® treated cells, sequestration of these metabolites in acidic organelles would prevent aglycones from interacting with the plasma membrane, where Pgp is localized.

## 4. Conclusions

In this report, we have demonstrated the ability of MEKC to assess differences in DOX metabolism between two drug delivery systems. A total of nine peaks associated with DOX metabolism were detected. Five peaks were common to both drug delivery systems, two appeared uniquely as a result of the Doxil® treatment, and two correspond to the treatment with free doxorubicin. Peak areas indicate that DOX is present at attomole levels per cell for the Doxil® treated and free DOX treated cells, while metabolites are detected at sub-attomole levels per cell. Unique metabolites are only present after treatment with Doxil® (metabolites 9 and 10), as well as two that were unique to free DOX treatment (metabolite 3 and 5), indicating the choice of drug delivery system influences the formation of metabolites in whole cell lysate. Using the MEKC separation technology described here, it was possible to conclude that the use of liposomes results in an increased relative accumulation of DOX metabolites as compared to free DOX in solution.

Since subcellular metabolite profiling may provide more specific information on the origin and fate of DOX metabolites formed under a given treatment, future work will focus on the subcellular analysis of metabolite profiles. In conjunction with subcellular analysis, identification of metabolites produced upon treatment by HPLC–MS may further explain how different drug delivery systems leads to unique intracellular metabolic profiles.

## Acknowledgements

This work has been supported by NIH R01-GM61969. We also wish to thank Dr. Antonio Suarato, Pharmacia, for his kind donation of doxorubicin.

## References

[1] L. Gallois, M. Fiallo, A. Garnier-Suillerot, Biochim. Biophys. Acta 1370 (1998) 31.
[2] D.C. Drummond, O. Meyer, K. Hong, D.B. Kirpotin, D. Papahadjopoulos, Pharmacol. Rev. 51 (1999) 691.
[3] C.M. Palmeira, J. Serrano, D.W. Kuehl, K.B. Wallace, Biochim. Biophys. Acta 1321 (1997) 101.
[4] G. Sacco, R. Giampietro, E. Salvatorelli, P. Menna, N. Bertani, G. Graiani, F. Animati, C. Goso, C.A. Maggi, S. Manzini, G. Minotti, Br. J. Pharmacol. 139 (2003) 641.
[5] J.M. Saul, A. Annapragada, J.V. Natarajan, R.V. Bellamkonda, J. Control Release 92 (2003) 49.
[6] S.S. Davis, I.M. Hunneyball, L. Illum, J.H. Ratcliffe, A. Smith, C.G. Wilson, Drugs Exp. Clin. Res. 11 (1985) 633.
[7] A. Gabizon, in: F.H.D. Roerdink, A.M. Kron (Eds.), Drug Carrier Systems, John Wiley & Sons, Chichester, 1989, p. 330.
[8] G.J. Charrois, T.M. Allen, Biochim. Biophys. Acta 1609 (2003) 102.
[9] A. Gabizon, D. Goren, R. Cohen, Y. Barenholz, J. Control Release 53 (1998) 275.
[10] C.A. Frederick, L.D. Williams, G. Ughetto, G.A. van der Marel, J.H. van Boom, A. Rich, A.H. Wang, Biochemistry 29 (1990) 2538.
[11] S. Licata, A. Saponiero, A. Mordente, G. Minotti, Chem. Res. Toxicol. 13 (2000) 414.
[12] M. Palumbo, B. Gatto, S. Moro, C. Sissi, G. Zagotto, Biochim. Biophys. Acta 1587 (2002) 145.
[13] A. Bodley, L.F. Liu, M. Israel, R. Seshadri, Y. Koseki, F.C. Giuliani, S. Kirschenbaum, R. Silber, M. Potmesil, Cancer Res. 49 (1989) 5969.
[14] K. Barabas, J.A. Sizensky, W.P. Faulk, J. Biol. Chem. 267 (1992) 9437.
[15] I. Pastan, M.M. Gottesman, Annu. Rev. Med. 42 (1991) 277.
[16] M.E. Clementi, B. Giardina, E. Di Stasio, A. Mordente, F. Misiti, Anticancer Res. 23 (2003) 2445.
[17] R.D. Arnold, J.E. Slack, R.M. Straubinger, J. Chromatogr. B 808 (2004) 141.
[18] D.L. Chin, B.L. Lum, B.I. Sikic, J. Chromatogr. B 779 (2002) 259.
[19] S. Fogli, R. Danesi, F. Innocenti, A. Di Paolo, G. Bocci, C. Barbara, M. Del Tacca, Ther. Drug Monit. 21 (1999) 367.
[20] A.B. Anderson, E.A. Arriaga, J. Chromatogr. B 808 (2004) 295.
[21] A.B. Anderson, J. Gergen, E.A. Arriaga, J. Chromatogr. B 769 (2002) 97.
[22] A.B. Anderson, C.M. Ciriacks, K.M. Fuller, E.A. Arriaga, Anal. Chem. 75 (2003) 8.
[23] M.A. Le Bot, J.M. Begue, D. Kernaleguen, J. Robert, D. Ratanasavanh, J. Airiau, C. Riche, A. Guillouzo, Biochem. Pharmacol. 37 (1988) 3877.
[24] D.L. Gustafson, J.C. Rastatter, T. Colombo, M.E. Long, J. Pharm. Sci. 91 (2002) 1488.
[25] D.M. Pinto, E.A. Arriaga, D. Craig, J. Angelova, N. Sharma, H. Ahmadzadeh, N.J. Dovichi, Anal. Chem. 69 (1997) 3015.
[26] C.F. Duffy, S. Gafoor, D.P. Richards, H. Admadzadeh, R. O'Kennedy, E.A. Arriaga, Anal. Chem. 73 (2001) 1855.
[27] S. Takanashi, N.R. Bachur, Drug Metab. Dispos. 4 (1976) 79.
[28] X.F. Li, H. Ren, X. Le, M. Qi, I.D. Ireland, N.J. Dovichi, J. Chromatogr. A 869 (2000) 375.
[29] C.M. Boone, J.P. Franke, R.A. de Zeeuw, K. Ensing, J. Chromatogr. A 838 (1999) 259.
[30] R.J. Green, T.J. Su, J.R. Lu, J.R.P. Webster, J. Phys. Chem. B 105 (2001) 9331.
[31] B. Verzola, C. Gelfi, P.G. Righetti, J. Chromatogr. A 868 (2000) 85.
[32] D.J. Bailey, J.G. Dorsey, J. Chromatogr. A 852 (1999) 559.
[33] P. Camilleri, G.N. Okafo, J. Chem. Soc. Chem. Commun. 7 (1992) 530.
[34] M.H. Gaber, K. Hong, S.K. Huang, D. Papahadjopoulos, Pharm. Res. 12 (1995) 1407.
[35] S. Ning, K. Macleod, R.M. Abra, A.H. Huang, G.M. Hahn, Int. J. Radiat Oncol. Biol. Phys. 29 (1994) 827.
[36] O. Bakouche, D. Gerlier, J. Microencapsul. 2 (1985) 39.
[37] E. Bolotin, R. Cohen, L. Bar, N. Emanuel, S. Ninio, D. Lasic, Y. Barenholz, J. Liposome Res. 4 (1994) 455.
[38] X. Li, D. Hirsch, D. Cabral-Lilly, A. Zirkel, S. Gruner, A. Janoff, W. Perkins, Biochim. Biophys. Acta 1415 (1998) 23.
[39] E. Goormaghtigh, P. Huart, M. Praet, R. Brasseur, J.M. Ruysschaert, Biophys. Chem. 35 (1990) 247.
[40] G. Speelmans, R.W. Staffhorst, K. Versluis, J. Reedijk, B. de Kruijff, Biochemistry 36 (1997) 10545.

[41] M.A. Roberts, L. Locascio-Brown, W.A. MacCrehan, R.A. Durst, Anal. Chem. 68 (1996) 3434.
[42] S.P. Radko, M. Stastna, A. Chrambach, J. Chromatogr. B 761 (2001) 69.
[43] M.J. Kirchmeier, T. Ishida, J. Chevrette, T.M. Allen, J. Liposome Res. 11 (2001) 15.
[44] T.E. Murdter, G. Friedel, J.T. Backman, M. McClellan, M. Schick, M. Gerken, K. Bosslet, P. Fritz, H. Toomes, H.K. Kroemer, B. Sperker, J. Pharmacol. Exp. Ther. 301 (2002) 223.
[45] G. Razzano, V. Rizzo, A. Vigevani, Farmaco 45 (1990) 215.
[46] C.R. Yates, C. Chang, J.D. Kearbey, K. Yasuda, E.G. Schuetz, D.D. Miller, J.T. Dalton, P.W. Swaan, Pharm. Res. 20 (2003) 1794.